

CHAPTER 4

Host-guest Chemistry: Influence of n-octyl chain in the design strategy for penetrating organic bilayers

1-Octyl-3-methylimidazolium and 1-octyl-2,3-dimethylimidazolium cations forms multi-component solid state structures with p-sulfonatocalix[4]arene and/or large mono-phosphonium cations, as well as aquated lanthanide metal ions, with the imidazolium ring confined in the calixarene cavity, essentially forming 'molecular capsules' based on two calixarenes or with the imidazolium head group residing in the calixarene cavity while the terminus of the n-octyl chain penetrating the adjacent hydrophobic bilayer which is comprised of calixarenes with or without phosphonium ions. The nature of the calixarene-imidazolium interplay is mapped out using Hirshfeld surface analysis while the supermolecules in aqueous state is investigated using ^1H NMR.

4.1 Introduction

Increasing the alkyl side chain length in 1-alkyl-3-methylimidazolium cations from methyl to butyl gets into the realms of ionic liquids, depending on the nature of the anion. For the series from butyl to octyl, there is an increase in the hydrophobicity of the ionic liquid, along with an increase in viscosity, and a decrease in density and surface tension values due to the formation of Coulombic layers where the ionic head-groups interact with the counter ions, and van der Waals layers are built from the stacking of the alkyl chains ^[153, 186].

In aqueous solutions, ionic liquids have surface active properties similar to surfactants, which lead to self-organization into micelles or aggregates, depending on the alkyl chain length ^[187]. Imidazolium cations with short chain system can be modeled as polydispersed spherical aggregates, whereas the long chain system can be modeled as a system of regularly sized near-spherical charged micelle ^[188]. Addition of a certain amount of water to ionic liquids with long chains results in spontaneous self-organization into liquid-crystalline ionogels, where segregation of the hydrophilic and hydrophobic segments takes place, forming regions of confined water, ultimately with the onset of gelation ^[188-190].

Given the above effect of increasing the alkyl side chain length, the self assembly of 1-octyl-3-methylimidazolium, **8** and 1-octyl-3-dimethylimidazolium, **9** with symmetrical and unsymmetrical phosphonium cations and *p*-sulfonatocalix[4]arene, **1** has been investigated. Remarkably **8** and **9** forms four component complexes with the calixarene macrocycle **1**, phosphonium cations **10** or **11**, and aquated lanthanide metal ions as an unconventional bilayer arrangement ^[85]. The selectivity of the charged head group to reside in the cavity of the calixarene as a host-guest component is significant, as is the organic tail of the host-guest complex either penetrating the adjacent bilayer or

snugly fits in another calixarene. Hirshfeld surface ^[191, 192] analysis has also been undertaken to understanding the nature of interplay of the molecules in such complex self assembled systems.

4.2 Structural features involving 1-octyl-3-methylimidazolium and 1-octyl-3-dimethylimidazolium

4.2.1 Solid state structures based on 1-octyl-3-methylimidazolium complexes

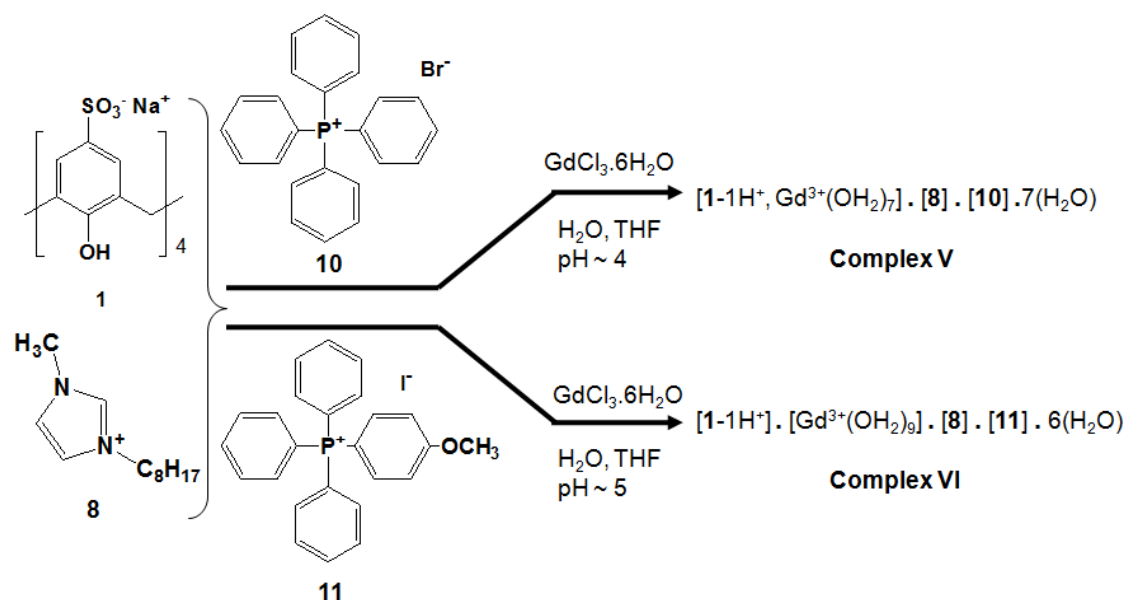


Figure 4.1. Synthesis of complexes **V** and **VI**.

Complexes **V** and **VI** were obtained from water/tetrahydrofuran (THF) by slow evaporation of an equimolar mixture of **1** and **8** and a three-fold excess of aqueous gadolinium(III) chloride, with phosphonium cations, **10** or **11**, as bromide and iodide salts respectively, Figure 4.1. Both complexes **V** and **VI** crystallise in the triclinic space group $P-1$, ($Z=2$) and each is built of calixarene anions, imidazolium cations, phosphonium cation, and lanthanide ions with coordinated water molecules, in the ratio 1:1:1:3, as well as water molecules filling up the voids in the extended structures. Complexes **V** and **VI** have conformationally restricted cone-shaped calix[4]arene in an

‘up–down’ antiparallel bilayer arrangements, with the lower rim hydroxyl groups arranged in a back-to-back manner with a distance between planes of the calixarenes at 1.73 Å and 2.66 Å for complexes **V** and **VI** respectively (the distance between planes is defined by the distance of the basal plane at the lower rim of calixarenes consisting of the four hydroxyl group O-centres relative to the adjacent calixarene basal plane). Electrical neutrality is achieved in the systems by the calixarenes taking on a 5- charge arising from the removal of one of the H-atoms on the lower rim of the calixarene, which has been noted in other systems^[119, 120]. Such charge on the calixarene usually leads to spheroidal like structures, in contrast to bilayer arrangements in the present structures, noting that spheroidal structures are formed in the absence of phosphonium cations^[119, 120].

The coordination of gadolinium(III) cation is different in the two structures. Complex **V** has a sulfonate group attached directly to the metal centre (Gd–O at 2.369(1) Å) with seven water molecules completing the coordination sphere (Gd–O at 2.353(1) to 2.443(1) Å), whereas complex **VI** has homoleptic metal centres devoid of coordinated sulfonate groups, being bound exclusively by nine water molecules (Gd–O at 2.364(6) to 2.515(6) Å). All water molecules are involved in a hydrogen bond network with O···O distances in the range of 2.647(2) to 3.323(2) Å (**V**) and 2.430(12) to 3.276(5) Å (**VI**). Some of the coordinated water molecules are in close proximity to the calixarene sulfonate groups, with short Gd–O···O contacts at 2.793(2) to 2.858(2) Å for complex **V**, and 2.703(4) to 2.829(14) Å for complex **VI**, which is consistent with hydrogen bonding interactions. The difference in the mode of coordination of the gadolinium cations to the calixarenes, either with a sulfonate group bound directly to the metal centre in **V**, or with the metal centre in **VI** being exclusively bound to water molecules results in a significant difference in the distance between the bilayers. In complex **V**, the packing between the bilayers is more compact, with a distance from the

centre of the bilayer to the next bilayer at 17.6 Å, Figure 4.2. This compares with the corresponding distance of 18.7 Å in complex **VI**, Figure 4.3.

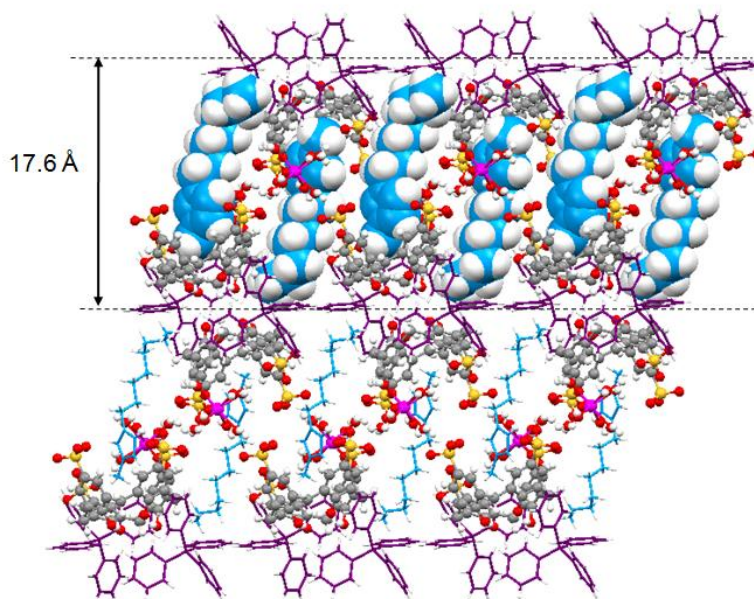


Figure 4.2. Projection down the *b*-axis with some space filling of imidazolium guest molecules (blue) confined in calixarenes, and layers of phosphonium cations (purple) in the extended bilayer of complex **V**. Crystalline water molecules were omitted for clarity.

Large phosphonium cations are embedded within the bilayers in a grid-like packing arrangement, Figure 4.4, in the common edge-to-face (**ef**) multiple phenyl embrace between molecules with distance between the P-atoms at 6.24 and 6.62 Å for complex **V** and **VI** respectively, Figure 4.5. The phosphonium cations in the calixarene bilayers are associated with the C–H··· π interaction as well as H-bonding with the oxygen containing fragments in the calixarene molecules and some coordinated water molecules at the gadolinium metal sphere. The thickness of the calixarene bilayer with embedded phosphonium cations is similar in both structures, at approximately 15.3 Å and 14.9 Å respectively for complex **V** and **VI**.

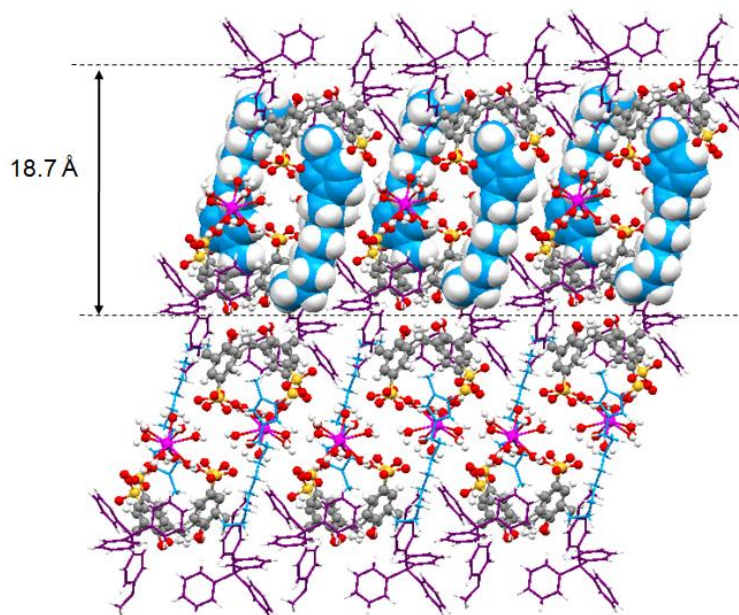


Figure 4.3. Projection down the *b*-axis of calixarene - imidazolium supermolecules in complex **VI** with some space filling of imidazolium guest molecules (blue) and layers of phosphonium cations (purple). Crystalline water molecules were omitted for clarity.

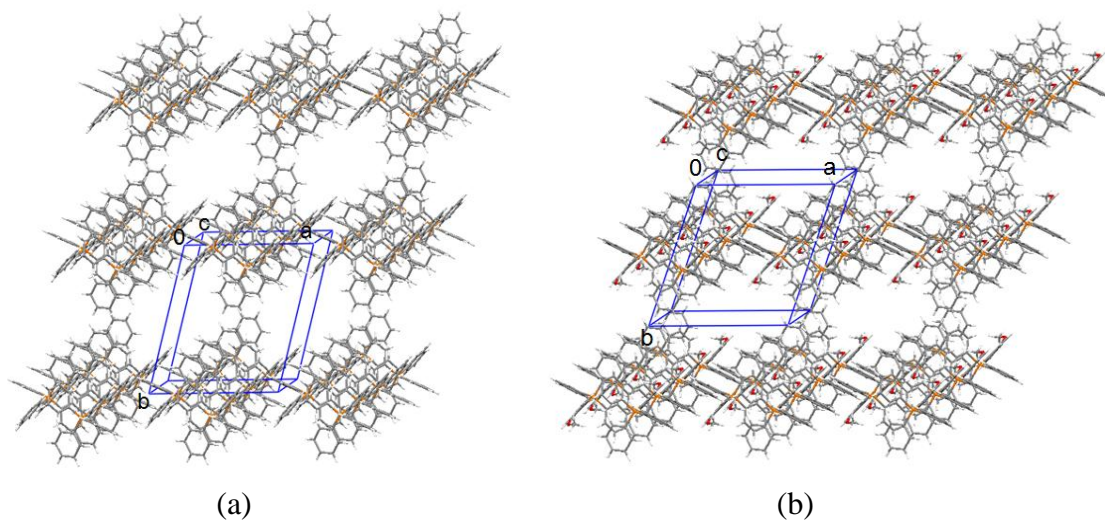


Figure 4.4. Stick representation of embedded phosphonium ions projected down *c*-axis in (a) complex **V** and (b) complex **VI**.

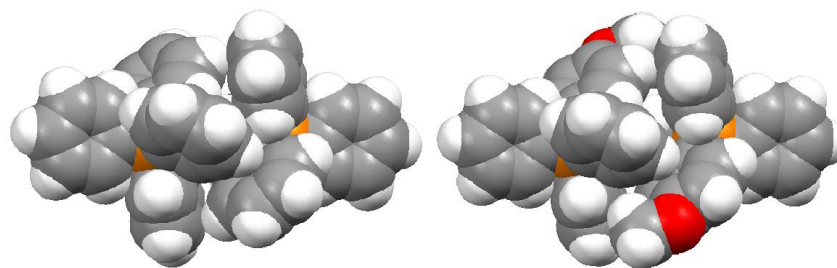


Figure 4.5. Multiple phenyl embraces of phosphonium paired molecules in complex **V** (left) and complex **VI** (right).

In both cases, the imidazolium cations are accommodated in the calixarene cavities with the long alkyl chains interacting with the hydrophobic segment within the compact bilayers. It is noteworthy that the octyl chain in complex **VI** is twisted relative to that in complex **V** which demonstrates the flexibility of this moiety in penetrating the bilayers. The twist presumably relates to the difference in the mode of coordination of the gadolinium(III) cations which is manifested in different thicknesses between the calixarene bilayers. In both structures, the tail of the octyl chain penetrates the bilayer to the same extent, but the overall distance from one calixarene to a calixarene in the next layer is different. In comparison, the distance from the calixarene basal plane defined by the four methylene bridges, to the C-atom in the octyl alkyl chain before any twisting in complex **V** is shorter than in complex **VI**, the distances being 12.1 and 14.1 Å respectively, Figure 4.6.

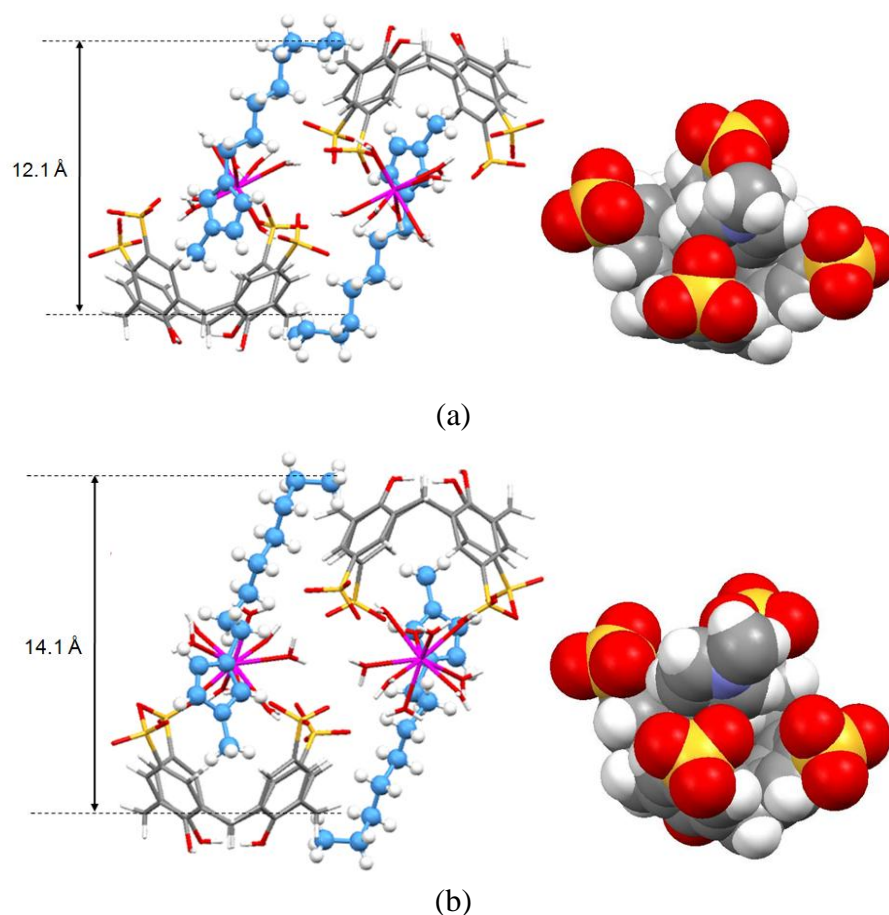


Figure 4.6. Close contacts for the calixarene - imidazolium supermolecules in complex **V** (a) and complex **VI** (b) with equivalent space-filling representation (right).

The complementarity of interaction of the cationic five membered imidazolium ring and nearest substituents with the calixarene cavity is evident, with the long alkyl chain protruding into the next bilayer having various weak intermolecular interactions with calixarenes, phosphonium cation and included crystalline water molecules. For both complexes, the imidazolium cation is selectively drawn into the calixarene with the methyl group directed into the cavity in a pinched cone conformation with angles between the plane of all four phenyl rings of the calixarene with respect to the basal plane consisting of four methylene bridges at $69.7(1)^\circ$, $42.1(1)^\circ$, $67.8(1)^\circ$, and $48.7(1)^\circ$ and $60.2(1)^\circ$, $52.7(1)^\circ$, $70.1(1)^\circ$ and $49.5(1)^\circ$ for complex **V** and **VI** respectively.

The methyl termini of the imidazolium cation in complex **V** has multiple close contacts involving: (i) C–H··· π interaction of methyl group to the phenyl rings of calixarene, with short distances at 2.56 and 2.64 Å (corresponding C··· π distances at 3.52 to 3.57 Å), (ii) C–H··· π interaction of an H-atom of the five member ring to a calixarene phenyl ring, at 2.55 Å (corresponding C··· π distances of 3.48 Å), and (iii) an H-atom of the five member ring having close C–H···O contacts with sulfonate group, with C–H···O distance at 2.51 Å (corresponding C···O distance at 3.36 Å). The H-atom of the five membered ring is also involved in the H-bonding network with the O-atom of crystalline water molecules, with the shortest contacts being 2.19 Å. The imidazolium cation in complex **VI** also has similar multiple close contacts involving: (i) C–H··· π interactions from the methyl group of the imidazolium and calixarene phenyl rings, at distances of 2.85 Å and 2.95 Å (corresponding C··· π distances of 3.74 to 3.57 Å), and (ii) an H-atom of the five member ring having close C–H···O contacts with a sulfonate group, with C–H···O distance at 2.46 Å (corresponding C···O distance at 3.37 Å). Crystalline water molecules and H-atoms of the imidazolium cation are involved in H-bonding interactions with the closest H···O contacts at 2.18 Å.

Multiple close contacts involving the octyl chain and calixarenes were identified with the octyl chain penetrating the next bilayer residing in between calixarenes. The imidazolium octyl chain in complex **V** has weak H-bond interactions involving (i) a C–H···O short distance at 2.42 Å (corresponding C···O distance at 3.25 Å) with an adjacent sulfonate group, and (ii) close C–H···H–C contacts at 2.31 and 2.38 Å (corresponding C···C distance at 4.12 and 4.20 Å) associated with a H-atom of a calixarene phenyl ring, and a H-atom from an adjacent calixarene methylene bridge. The terminal C-atom of the octyl chain nestles close to the methylene bridge of calixarene in the next bilayer at 3.99 Å (corresponding H···H distance at 2.26 Å). Close contacts of the octyl chain with calixarene in complex **VI** are: (i) C–H···O contacts at

2.37 and 2.62 Å (corresponding C...O distance at 3.15 and 3.54 Å) involving the adjacent sulfonate groups, (ii) a C–H...H–C close distance at 2.41 Å (corresponding C...C distance at 4.31 Å) involving an H-atom of calixarene phenyl ring, and (iii) C–H...H–C contacts at 2.49 and 2.74 Å (corresponding C...C distance at 4.05 and 4.31 Å) involving phosphonium H-atoms. The terminal C-atom of the octyl chain is close to a C-atom of the phenyl ring of a phosphonium cation, at 3.97 Å (corresponding H...H distance is 2.42 Å).

4.2.2 Hirshfeld surface analysis for structures based on 1-octyl-3-methyl-imidazolium complexes

Hirshfeld surface analysis reveals the close intermolecular interactions as bright red spots on the d_{norm} visualization surface with blue regions devoid of close contacts^[193]. Figure 4.7 shows the Hirshfeld surfaces for imidazolium cations with other components in close proximity to the cation. The red regions designated **1** and **2** in Figure 4.7 (a) and (b), identify the closest contacts associated with C–H...O interactions, and H...C interactions (*i.e.* C–H... π) between imidazolium cation and other components. The respective intermolecular interactions appear as distinct spikes in the fingerprint plots, Figure 4.8, labelled corresponding as **1**, ($d_e + d_i = 2.19$ Å for complex **5** and 2.18 Å for complex **V**) and **2** ($d_e + d_i = 2.56$ Å for complex **5** and 2.85 Å for complex **V**), similar to the calculated values discussed above. Spike **1** corresponds to the H-bonding network which is a donor spike (H-atoms of imidazolium cation interacting with O-atoms from the sulfonate group and water molecules), and is more intense than the H...H intermolecular interaction which primarily involves the H-atoms of the imidazolium cation in close proximity to water molecules and calixarene component (circled in red) for both structures. The wing at the upper left of the plot, **2**, highlight characteristic C–H... π donor interactions, involving the H-atom of imidazolium cation pointing towards

the calixarene phenyl rings. Complex **VI** has longer contacts compared with complex **V** with the imidazolium cation confined in a less dense packing and has a smaller amount of water molecules included in the structure and thus the contacts between atoms are much longer. The Hirshfeld surface analysis data further confirm the multicomponent close distances discussed above. A summary of all close contacts involving imidazolium cation and other components is shown as percentage constituents in Figure 4.9.

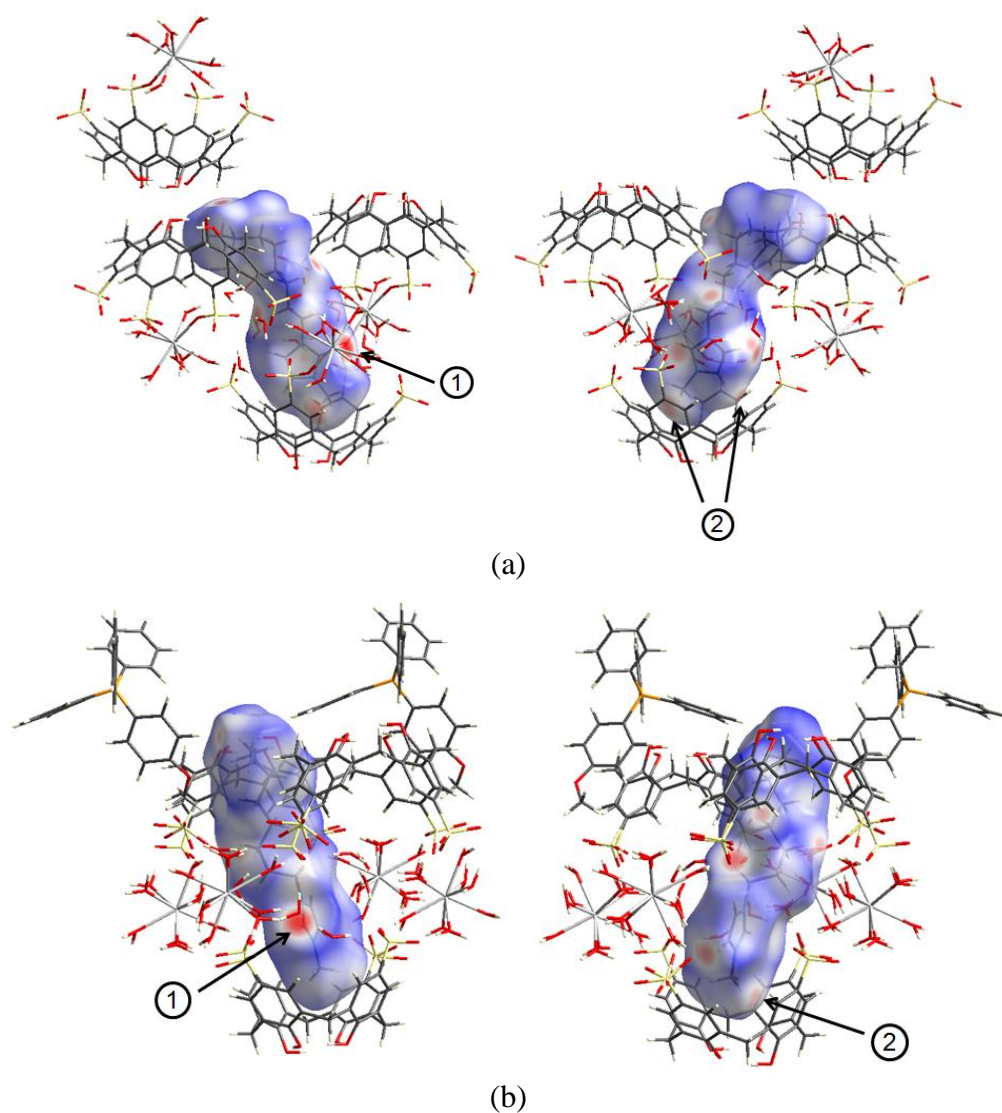


Figure 4.7. Hirshfeld surfaces for imidazolium cations (a) complex **V**, and (b) complex **VI** showing all close contacts of imidazolium cation and nearest components, with two views related by a 180° rotation about the vertical axis.

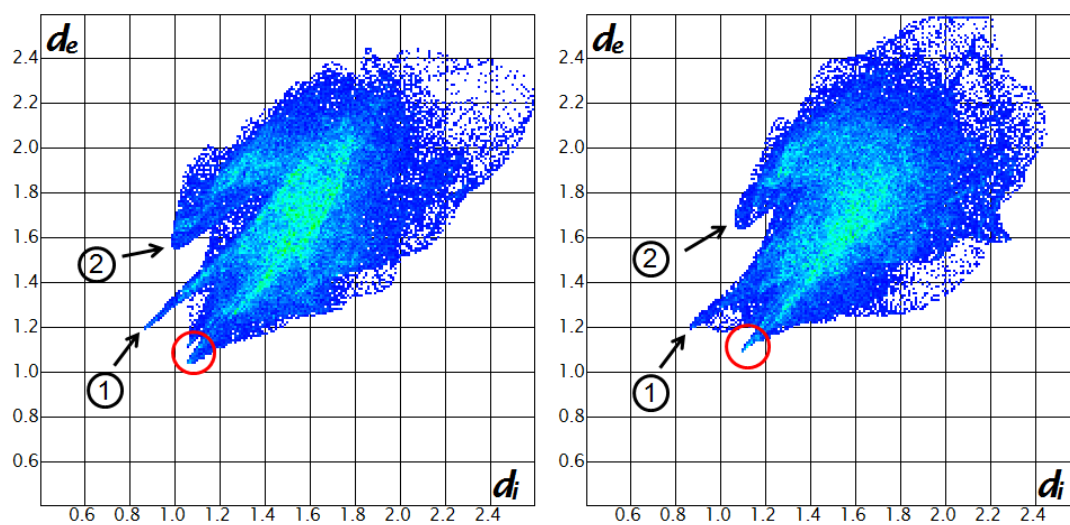


Figure 4.8. Fingerprint plots for complex **V** (left) and **VI** (right) showing regions of close intermolecular contacts.



Figure 4.9. Relative contributions to the Hirshfeld surface for the major intermolecular contacts associated with the imidazolium cations in complexes **V** and **VI**.

4.2.3 Solid state structures based on 1-octyl-3-dimethylimidazolium complexes

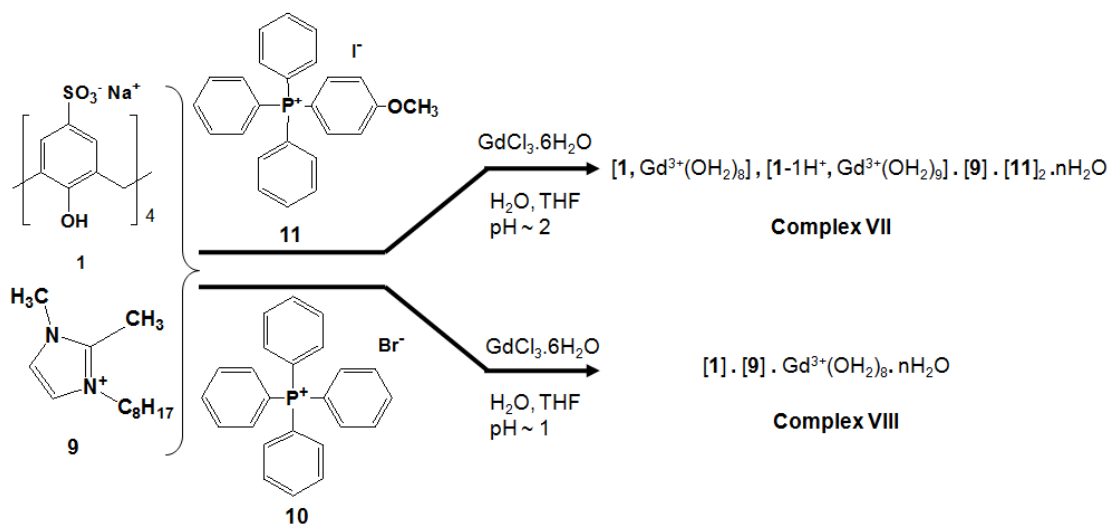


Figure 4.10. Synthesis of complexes **VII** and **VIII**.

Slow evaporation of equimolar mixtures of **1** and **9** and phosphonium salts, **10** or **11**, in the presence of a three-fold excess of aqueous gadolinium(III) in water/tetrahydrofuran (THF), afforded complexes **VII** and **VIII**, Figure 4.10. In both cases, the *n*-octyl dimethylimidazolium cation is selectively drawn into the calixarene cavity primarily through the N-methyl group. Both structures have a bilayer arrangement of calixarenes, with one arranged back-to-back and the other in an offset back-to-back manner, with and without incorporation of phosphonium cations, but the interplay of the bilayers is distinctly different. Complex **VII** can be considered as being built of ‘molecular capsules’ with the imidazolium cation encapsulated by two calixarenes with the alkyl chain bent. In contrast, complex **VIII** has the essentially straight long alkyl chain of the imidazolium cation penetrating the next calixarene bilayer.

Complex **VII** crystallises in the monoclinic space group $P2_1/m$, ($Z=2$), with the asymmetric unit comprising a *p*-sulfonatocalix[4]arene with an aquated gadolinium(III) cation, one *n*-octyl dimethylimidazolium cation distributed between two positions, and one phosphonium cation [(3-methoxyphenyl)triphenylphosphonium], along with half-populated disordered included water molecules. The calixarenes form ‘molecular

capsules', over inversion centres, although electrical neutrality requires one of them to take on a 4- charge and the other a 5- charge. Thus one proton has been removed from the lower rim of one of the calixarenes making up the walls of the 'capsules'. The homoleptic gadolinium(III) metal ions are located on a mirror plane with one forming a secondary coordination sphere with eight disordered water molecules while the other has nine water molecules. The metal ion interacts with the calixarene through hydrogen bonding, in the equator of 'molecular capsules', as judged by the close proximity of the O-atom of the sulfonate group to the aquated gadolinium cations, closest O...O distances being 2.529(1) to 2.883(2) Å. The disordered water molecules are involved in extended H-bonding with O...O distances in the range 2.622(8) to 3.061(6) Å.

In the extended structure, the 'molecular capsules' are embedded into the usual bilayers arrangement, Figure 4.11, with each 'capsule' shrouding one disordered imidazolium cation over two sites with equal population. The imidazolium charged head group is positioned within the calixarene cavity, with the calixarene pinching around the guest and the angles of all four phenolic rings with the basal plane of the four methylene bridges at the lower rim of calixarene are 51.11(1)°, 63.55(5), 45.18(6)°, and 63.06(4)°. The encapsulated imidazolium cations have multiple interactions with the walls of the capsules, namely weak H-bonding and C-H... π interaction, Figure 4.12. The charged head group of the dimethylimidazolium cation is involved in: (i) C... π (centroid) interactions from the methyl group to the phenyl ring of calixarene, with the C... ring centroid distance at 3.61 Å, and (ii) H-bonding to the calixarene sulfonate groups, with C-H...O distances ranging from 2.51 to 2.78 Å (corresponding C...O distances are 3.28 to 3.64 Å). The long aliphatic chain is distorted and resides in the calixarene cavity, with (i) C-H...O close contacts ranging from 2.30 to 2.81 Å (corresponding C...O distances are 3.21 to 3.79 Å), and (ii) C-H... π (centroid)

interaction to the phenyl ring of calixarene, with distances ranging from 2.64 to 2.74 Å (corresponding C···O distances are 3.56 to 3.63 Å).

The bilayer contains calixarenes and phosphonium cations which are in the common phenyl embrace arrangement in a grid-network, filling the interstices between the interfaces of calixarene hydroxyl groups with an overall bilayer thickness of 13.0 Å, Figure 4.11. The phosphonium cations have C··· π close contacts at 3.64 Å involving the interaction between the calixarene methylene bridge and the phenyl ring of phosphonium cation. The H-atoms on the phosphonium cations are also involved in weak H-bonding with O-atoms of the calixarene molecules, for both the sulfonate and hydroxyl groups, with short contacts from 2.60 to 2.70 Å and 2.86 Å (corresponding C···O distances are 3.44 to 3.45 Å and 3.72 Å) respectively. The ‘molecular capsules’ are approximately 18.4 Å in length along the principle axis, Figure 4.11.

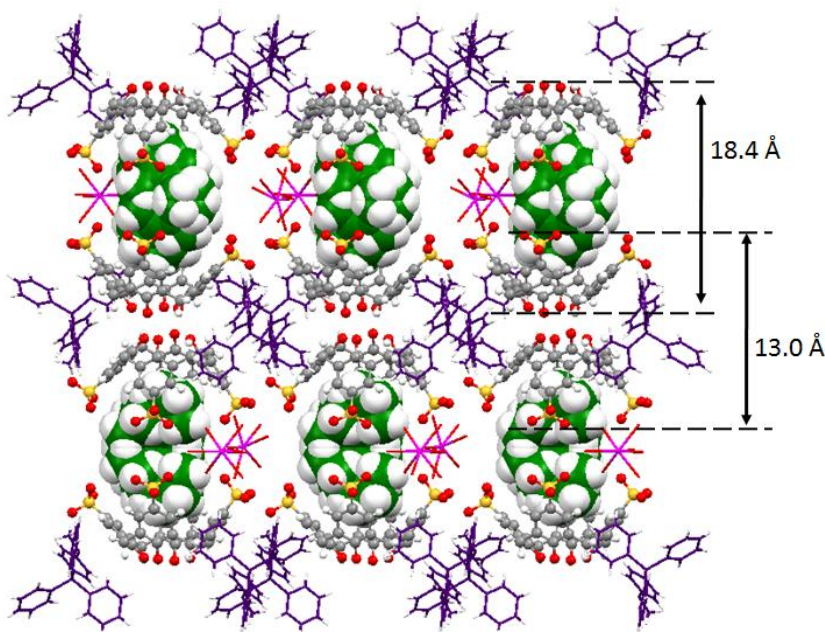


Figure 4.11. Projection of complex VII down *a*-axis showing the arrangement of *n*-octyl dimethylimidazolium cations (green) encapsulated in the ‘capsules’ of calixarenes.

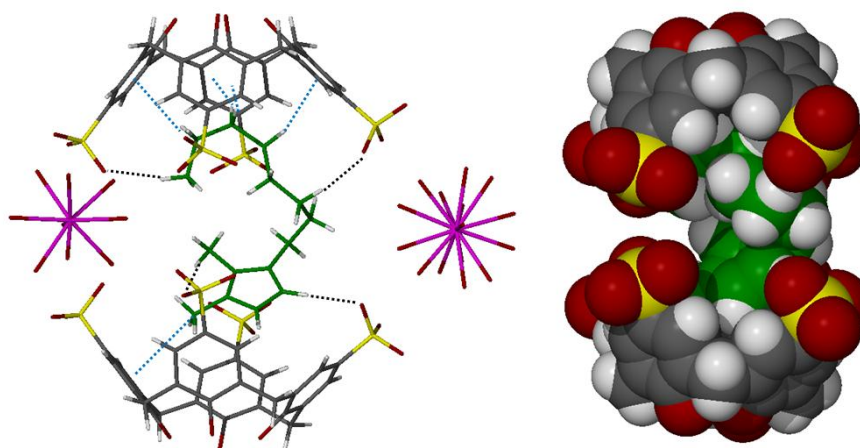


Figure 4.12. Arrangement of *n*-octyl dimethylimidazolium cation in the ‘molecular capsule’ in complex **VII**, showing nearest contacts (left) and the corresponding space filling (right). The disordered parts of the imidazolium cation are omitted for clarity.

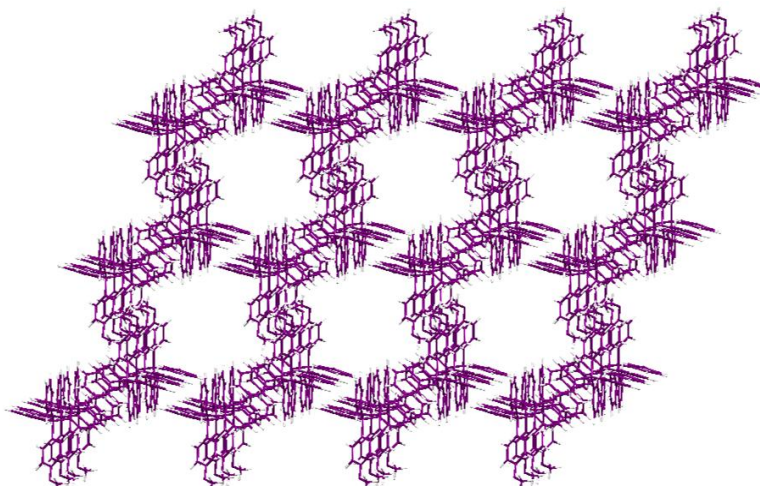


Figure 4.13. Stick representation of embedded phosphonium molecules projected along the *b*-axis in complex **VII**.

Complex **VIII** crystallises in the triclinic space group $P-1$, ($Z=2$), with the asymmetric unit comprised of one calix[4]arene, one imidazolium cation and one gadolinium(III) cation, which has a secondary coordination sphere through hydrogen bonding with the calixarenes and included water molecules. The homoleptic metal ion is coordinated by eight water molecules, and has close contacts with the sulfonate groups of the calixarene through extensive hydrogen bonding, the Gd–O \cdots O distances ranging from 2.684(2) Å to 2.840(1) Å. The crystalline water molecules in the extended structure are involved in a H-bonding network with O \cdots O distances in the range of 2.687(2) to 2.902(2) Å.

In complex **VIII**, the large phosphonium cations are absent in the structures which is reflected in a significant difference in the distance between the bilayers, with a more compact inter layer, 14.7 Å thick, and bilayer, 9.67 Å thick, Figure 4.14. In the previous structures based on *n*-octyl imidazolium (complex **V** and **VI**), the bilayer thickness is much larger, which relates to the incorporation of the positively charged phosphonium cations within the bilayers. The *n*-octyl dimethylimidazolium cation in the present study fits tightly in the calixarene cavity in the pinched cone configuration (the angles between the plane of all four phenyl rings of the calixarene with respect to the basal plane consisting of four methylene bridges are 73.02(4) $^\circ$, 37.33(4) $^\circ$, 71.61(4) $^\circ$, and 42.14(4) $^\circ$), Figure 4.14, with the long alkyl chains in contact with a neighbouring calixarene molecule, and penetrating the adjacent bilayer. The flexibility of the *n*-octyl is demonstrated with the alkyl chain being slightly twisted in being accommodated into the tightly packed bilayer.

The *n*-octyl dimethylimidazolium ring resides in the calixarene cavity, through (i) C \cdots π interactions of the methyl groups and the phenyl rings of the calixarene, with close distances ranging from 3.32 to 3.33 Å, and (ii) C–H \cdots O interactions between H-atoms of the cation and calixarene sulfonate groups, with C–H \cdots O distances ranging

from 2.64 to 2.72 Å (corresponding C···O distances are 3.19 to 3.32 Å). Multiple close contacts involving the *n*-octyl chain and neighbouring calixarene are evident with the octyl chain penetrating the next bilayer, in between calixarenes, with (i) C–H···O contacts at 2.74 and 2.93 Å (corresponding C···O distances are 3.46 and 3.90 Å) for adjacent sulfonate groups, and (ii) C–H···H–C contacts ranging from 2.49 to 2.58 Å (corresponding C···C distances are 3.95 to 4.35 Å) for H-atoms on the calixarene molecules. The terminal C-atom of the octyl chain nestles close to a methylene bridge of calixarene in the next bilayer at 4.18 Å (corresponding H···H distance 3.49 Å).

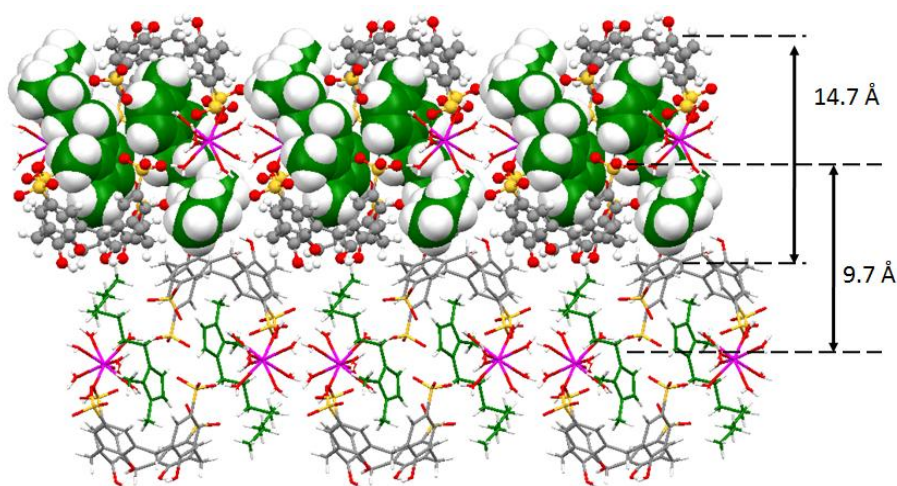


Figure 4.14. Projection of the extended structure in complex **VIII** down the *a*-axis, with some space filling of the imidazolium cations (green).

4.2.4 Hirshfeld surface analysis for structures based on 1-octyl-3-dimethylimidazolium complexes

Visualization of close intermolecular interactions between the molecules in the solid state was undertaken using Crystal Explorer 2.1^[194]. The parameter d_{norm} in the Hirshfeld surface analysis is of particular interest, which displays a surface with a red-white-blue colour scheme; bright red spots for contacts shorter than the sum of their van der Waals radii, while blue regions are devoid of close contacts^[195]. Figure 4.15(a) and

6(c) show the Hirshfeld surfaces for both calixarene anion and dimethylimidazolium cation for complex **VIII**. The Hirshfeld surface analysis was not undertaken for complex **VII** because of the disorder fragment associated with the dimethylimidazolium cation.

The red regions (with yellow arrows pointing) identify the closest contacts associated with $\text{H}\cdots\text{C}$ interactions (*i.e.* $\text{C}-\text{H}\cdots\pi$) between dimethylimidazolium cation and calixarene. In the fingerprint plots, the area circled in yellow correspond to the $\text{C}-\text{H}\cdots\pi$ interaction with $d_e + d_i = 2.5 \text{ \AA}$, and the wing at the upper left of the plot, Figure 4.15 (d), highlights the characteristic $\text{C}-\text{H}\cdots\pi$ donor interactions involving the H-atom of imidazolium cation pointing towards the calixarene phenyl rings (centroids), making up 16% of the Hirshfeld surface. Three distinct spikes in the fingerprint plot Figure 4.15 (b) are evident, resulting from the weak H-bonding interactions and are identified as red regions (green arrows) in Figure 4.15 (a) and 4.15 (c). The spike (circled in green), results from close $\text{C}-\text{H}\cdots\text{O}$ contacts, principally from the dimethylimidazolium H-atoms in close proximity to calixarene sulfonate groups, making up 26% of the Hirshfeld surface. While the outermost spikes in the same plot (circled in red) represent $\text{O}\cdots\text{H}$ hydrogen bonding interactions, with the lower spike being the acceptor spike (O-atoms from the calixarene interacting with H-atoms from water molecules), and the upper spike is the donor spike (H-atoms from calixarene interacting with O-atoms from water molecules).

The fingerprint plots for *n*-octyl dimethylimidazolium are similar in shape to the *n*-octyl methylimidazolium, but there are differences between the structures. These relate to the arrangement of *n*-octyl methylimidazolium molecules in the cavity of calixarenes, and the shorter closest $\text{C}-\text{H}\cdots\pi$ and $\text{C}-\text{H}\cdots\text{O}$ interactions, noting the imidazolium ring in the present study has a C-methyl substitution.

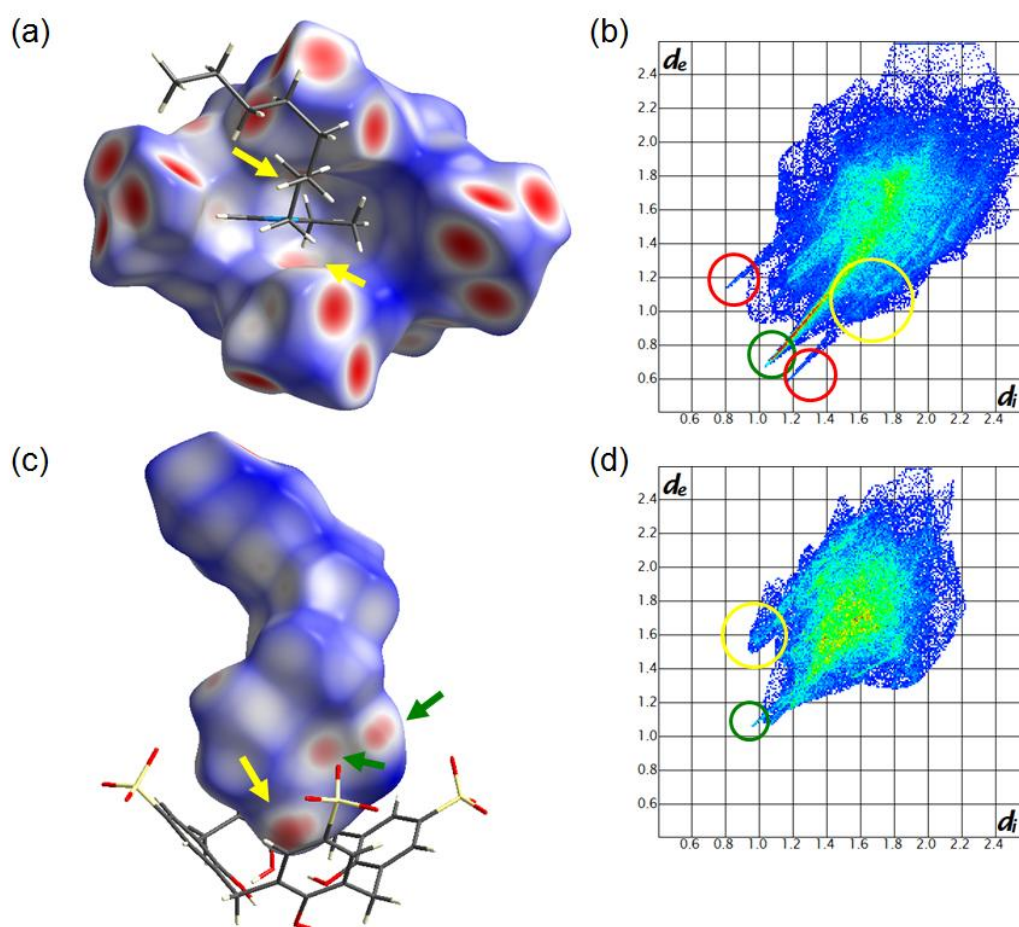


Figure 4.15. Hirshfeld surfaces for (a) calixarene and (c) dimethylimidazolium molecules for complex **VIII**, showing all close contacts of dimethylimidazolium cation and calixarene, with their respective fingerprint plots (b & d).

4.3 Solution studies involving 1-octyl-3-dimethylimidazolium complexes

The interplay of the *n*-octyl dimethylimidazolium cation and *p*-sulfonatocalix[4]arene was examined using ^1H NMR at 25°C in D_2O , for a 1:1 mixture of the two species Figure 4.16. This shows that the two components indeed form supermolecules in solution, [1-octyl-2,3-dimethylimidazolium \cap *p*-sulfonatocalix[4]arene], rather than the interplay of the two components in the solid

state being associated with crystal packing. The imidazolium BF_4^- salt has limited solubility in water for greater than a 1:1 mixture with the calixarene, and determining a binding constant was not possible, and the system is likely to be complicated by complex micelle formation. In this context it is noteworthy that in the ionic liquid–water system, the imidazolium based ionic liquids with long alkyl chains on the imidazolium ring can initiate phase separation^[150].

As to the formation of supermolecules, the upfield chemical shifts experienced by the N-methyl ($\text{H}\gamma$), the closest carbon atom of *n*-octyl ($\text{H}\beta$), and the unique H-atom ($\text{H}\delta$), as well as for the aromatic protons of the five membered ring protons ($\text{H}\alpha_1$ and $\text{H}\alpha_2$) is consistent with the dimethylimidazolium five membered ring residing in the cavity of the macrocycle. The protons of the hydrophobic aliphatic chain of the cation have minimum chemical shifts. Thus the NMR results confirm the formation of the supermolecule of calixarene and dimethylimidazolium, [1-octyl-2,3-dimethylimidazolium \cap *p*-sulfonatocalix[4]arene], rather than a ‘capsule’ with both the head group and long alkyl chain in its confines, and thus shielding effect, of the calixarenes. Rapid exchange on the NMR time scale with respect to the imidazolium head group residing in the calixarene cavity is evident with a change in chemical shifts with change in ratio of the two components, and that the calixarene is conformational mobile with the appearance of a broad peak for the methyl protons, at 3.85 ppm. Competition experiments between the imidazolium cation and a phenyl ring of the phosphonium cation residing in the calixarene cavity was not possible due to limited solubility of the phosphonium salts in water.

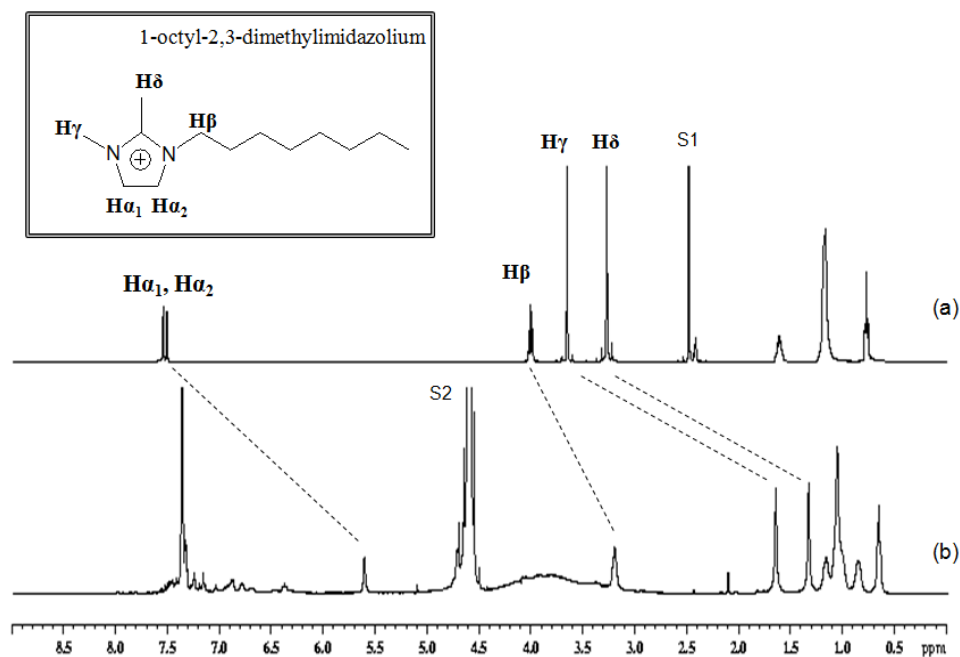


Figure 4.16. ^1H NMR spectrum for (a) *n*-octyl dimethylimidazolium and (b) *n*-octyl dimethylimidazolium in *p*-sulfonatocalix[4]arene (1:1), measured in DMSO (S1) and D_2O (S2).

4.4 Conclusions

Supramolecular assemblies incorporating *n*-octyl methylimidazolium and *n*-octyl dimethylimidazolium cations in *p*-sulfonated calix[4]arene system afforded four novel structures which depend on the nature of the phosphonium cations. The interplay of the five-membered ring is rather similar for all complexes, notably with the methyl terminal alkyl chain residing in the calixarene cavity. The calixarenes are organised into the common bilayers, linked by the gadolinium(III) metal centre with either the imidazolium cation confined in the calixarene cavity, or the terminal *n*-octyl chain penetrates into the adjacent bilayer. A remarkable finding is the incorporation or otherwise of phosphonium cations into the bilayer itself, by adding a simple substituent on the *para*-position of one of the phenyl rings in tetraphenyl phosphonium cation. The consequence of incorporating a C-methyl group on the *n*-octyl dimethylimidazolium

cation offers additional weak H-bond interaction between the H-atoms and the O-atoms of the calixarene sulfonate groups.

In now having studied the host-guest chemistry of *p*-sulfonated calix[4]arene with a series of imidazolium cations, a level of predicting the nature of the structures is now possible with the preferential binding of the calixarene towards smaller charged molecules of imidazolium cations rather than phenyl rings of large organic cations^[125]. This suggests that the use of longer alkyl chain analogues, is a valuable design strategy in constructing new organic bilayer arrangements where the long alkyl chain can penetrate an adjacent bilayer. The formation of bilayers is ubiquitous, but controlling the inclusion of phosphonium cations within the bilayers is a challenge.

The nature of the interplay of the four component systems is more easily understood using Hirshfeld surface analysis, with the results further highlighting the power of the technique in mapping out the interactions in a complex system, and how the components come together with complementary interactions.

4.5 Experimental Section

A. General remarks on crystal growth

p-Sulfonatocalix[4]arene sodium salt, **1**, was synthesised as described in Section 3.4. 1-octyl-3-methylimidazolium chloride, **8**, and 1-octyl-2,3-dimethylimidazoliumtetrafluoroborate salt, **9**, were synthesized according to the literature procedures^[141,196]. [Ph₄P]Br and [Ph₃PPhOMe]I, (**10** and **11**), were purchased from Sigma Aldrich. A hot solution of GdCl₃·6H₂O in water (0.5 mL) was added to a hot solution of phosphonium salt with *p*-sulfonatocalix[4]arene in a mixture of THF and water (1:1, 2 mL). The resulting solutions were left to cool and then allowed to slowly evaporate with crystals formed after several days. All NMR spectra were collected on a Varian 400 MHz spectrometer using D₂O at 25°C. The chemical shift changes of all the proton signals of the dimethylimidazolium were analyzed.

B. Synthesis of 1-octyl-3-methylimidazolium chloride

Excess of 1-chlorooctane were added to 1-methylimidazole were added in a round-bottomed flask fitted with a reflux condenser for 24 to 72 h at 70°C with vigorous stirring. The top phase containing unreacted starting material was decanted and the bottom phase was washed twice with ethyl acetate to remove any unreacted material. The product was dried under vacuum at 80°C and characterised by ¹H NMR (300MHz, D₂O) δ: 7.4 (d, 1H), 7.3 (d, 1H), 5.3 (s, 1H), 4.1 (t, 2H), 3.8 (s, 3H), 1.7 (m, 2H), 1.1 (m, 10H), 0.7 (t, 3H).

C. Synthesis of 1-octyl-2,3-dimethylimidazolium tetrafluoroborate

The 1-octyl-2,3-dimethylimidazolium chloride was vigorously stirred for 24 hours at room temperature with sodium tetrafluoroborate in distilled water solution. Phase separation will appear and the upper aqueous phase was decanted off while the ionic liquid phase was further dissolved in dichloromethane. The mixture was washed several times with water. The remaining solvents were removed using reduced pressure for 24 hours in an oil bath at 80°C attached to a high vacuum line. The product was characterised by ^1H NMR (300MHz, D_2O) δ : 7.6 (d, 1H), 7.5 (d, 1H), 4.0 (t, 2H), 3.7 (s, 3H), 3.3 (s, 3H), 1.7 (m, 2H), 1.2 (m, 10H), 0.7 (t, 3H).

D. Crystallography details

X-ray Crystallography

All data were measured as described in Section 3.4.

Crystal/refinement details for complex V:

$(\text{C}_{28}\text{H}_{33}\text{GdO}_{23}\text{S}_4)^{2-}, \text{C}_{24}\text{H}_{20}\text{P}^+, \text{C}_{12}\text{H}_{23}\text{N}_2^+, 7(\text{H}_2\text{O}), \text{C}_{64}\text{H}_{90}\text{GdN}_2\text{O}_{30}\text{PS}_4$, $M = 1683.84$, colorless plate, $0.29 \times 0.20 \times 0.08 \text{ mm}^3$, $a = 14.1299(3)$, $b = 15.0607(2)$, $c = 18.9204(3) \text{ \AA}$, $\alpha = 95.725(1)$, $\beta = 108.508(2)$, $\gamma = 102.781(2)^\circ$, $V = 3660.09(11) \text{ \AA}^3$, $Z = 2$, $D_c = 1.528 \text{ g/cm}^3$, $\mu = 1.128 \text{ mm}^{-1}$, $F_{000} = 1742$, $2\theta_{\text{max}} = 65.5^\circ$, 105256 reflections collected, 25096 unique ($R_{\text{int}} = 0.0395$). Final $Goof = 1.006$, $|\Delta\rho_{\text{max}}| = 1.7(1) \text{ e \AA}^{-3}$, $RI = 0.0324$, $wR2 = 0.0771$, R indices based on 19965 reflections with $I > 2\sigma(I)$, 919 parameters, 0 restraints. CCDC number: 725908.

Crystal/refinement details for complex VI:

$C_{28}H_{19}O_{16}S_4^{5-}, C_{25}H_{22}OP^+, C_{12}H_{23}N_2^+, GdH_{18}O_9^{3+}, 6(H_2O), C_{65}H_{94}GdN_2O_{32}PS_4, M = 1731.88$, colorless prism, $0.51 \times 0.24 \times 0.12 \text{ mm}^3$, $a = 14.3621(2)$, $b = 14.4461(2)$, $c = 19.9814(3) \text{ \AA}$, $\alpha = 99.588(1)$, $\beta = 104.357(1)$, $\gamma = 106.150(1)^\circ$, $V = 3732.08(9) \text{ \AA}^3$, $Z = 2$, $D_c = 1.541 \text{ g/cm}^3$, $\mu = 1.111 \text{ mm}^{-1}$, $F_{000} = 1794$, $2\theta_{\max} = 64.7^\circ$, 92489 reflections collected, 24538 unique ($R_{\text{int}} = 0.0355$). Final $Goof = 1.008$, $|\Delta\rho_{\max}| = 3.8(2) \text{ e \AA}^{-3}$, $RI = 0.0698$, $wR2 = 0.1970$, R indices based on 18807 reflections with $I > 2\sigma(I)$, 943 parameters, 7 restraints. CCDC number: 725909.

Crystal/refinement details for complex VII:

$C_{28}H_{20}O_{16}S_4^{4-}, C_{28}H_{19}O_{16}S_4^{5-}, 2(C_{25}H_{22}OP^+), GdO_8H_{16}^{3+}, GdO_9H_{18}^{3+}, C_{13}H_{25}N^+, 14(H_2O), C_{119}H_{170}Gd_2N_2O_{65}P_2S_8, M = 3301.49$, colorless rod, $0.36 \times 0.16 \times 0.15 \text{ mm}^3$, $a = 14.2968(2)$, $b = 36.8876(3)$, $c = 14.6319(2) \text{ \AA}$, $\beta = 110.886(1)^\circ$, $V = 7209.45(15) \text{ \AA}^3$, $Z = 2$, $D_c = 1.521 \text{ g/cm}^3$, $\mu = 1.146 \text{ mm}^{-1}$, $F_{000} = 3408$, $2\theta_{\max} = 64.8^\circ$, 182632 reflections collected, 24970 unique ($R_{\text{int}} = 0.0812$). Final $Goof = 1.002$, $|\Delta\rho_{\max}| = 3.3(2) \text{ e \AA}^{-3}$, $RI = 0.0909$, $wR2 = 0.2241$, R indices based on 16522 reflections with $I > 2\sigma(I)$, 871 parameters, 33 restraints. CCDC number: 749002.

Crystal/refinement details for complex VIII:

$C_{28}H_{20}O_{16}S_4^{4-}, C_{13}H_{25}N^+, Gd(OH_2)_8^{3+}, 5(H_2O), C_{41}H_{71}GdN_2O_{29}S_4, M = 1341.49$, colorless prism, $0.41 \times 0.34 \times 0.14 \text{ mm}^3$, $a = 13.2450(2)$, $b = 14.6552(3)$, $c = 15.3003(3) \text{ \AA}$, $\alpha = 103.867(2)$, $\beta = 100.692(1)$, $\gamma = 98.878(1)^\circ$, $V = 2771.10(9) \text{ \AA}^3$, $Z = 2$, $D_c = 1.608 \text{ g/cm}^3$, $\mu = 1.438 \text{ mm}^{-1}$. $F_{000} = 1382$, $2\theta_{\max} = 74.5^\circ$, 63423 reflections collected, 27437 unique ($R_{\text{int}} = 0.0249$). Final $Goof = 1.005$, $|\Delta\rho_{\max}| = 3.4(1) \text{ e \AA}^{-3}$, $RI = 0.0323$, $wR2 = 0.0819$, R indices based on 22954 reflections with $I > 2\sigma(I)$, 701 parameters, 0

restraints. CCDC number: 749003.